

Sensory neuropeptide CGRP and its co-receptor RAMP1 drive tumour cell growth in gastrointestinal cancers

Pavitha Parathan,^{1,2,3} Kelly Tran,^{1,2,3} Liam Neil,^{1,2} Tao Tan,^{4,5} Annalisa L E Carli,^{1,2} Yang Liao,^{1,2,6} Dmitri Mouradov,^{4,5} Jessica Da Gama Duarte ,^{1,2,7} Anne Huber,^{1,2} Bhupinder Pal,^{1,2} Peter Gibbs,^{4,5} Oliver M Sieber,^{4,5,8,9} Isaac M Chiu,¹⁰ Conor J Kearney,^{1,2} Wei Shi,^{1,2,6} John M Mariadason,^{1,2} David S Williams,^{1,2,11} Michael Buchert,^{1,2} Lisa A Mielke ^{1,2,3}

To cite: Parathan P, Tran K, Neil L, *et al*. Sensory neuropeptide CGRP and its co-receptor RAMP1 drive tumour cell growth in gastrointestinal cancers. *BMJ Oncology* 2025;4:e000842. doi:10.1136/bmjonc-2025-000842

► Additional supplemental material is published online only. To view, please visit the journal online (<https://doi.org/10.1136/bmjonc-2025-000842>).

Received 20 April 2025
Accepted 19 September 2025



© Author(s) (or their employer(s)) 2025. Re-use permitted under CC BY-NC. No commercial re-use. See rights and permissions. Published by BMJ Group.

For numbered affiliations see end of article.

Correspondence to
Dr Lisa A Mielke;
lisa.mielke@onjcri.org.au

ABSTRACT

Objective The gastrointestinal (GI) tract is densely innervated, forming a critical network that secretes neuropeptides essential for gut function. Tumour cells are highly adaptive and exploit their microenvironment, including nerves, to support and accelerate growth. However, the mechanisms by which tumour cells interact with neuropeptides in human GI cancers remain poorly understood. We aimed to investigate the expression and function of the sensory neuropeptide calcitonin gene-related peptide (CGRP) and its receptor component, receptor activity-modifying protein 1 (RAMP1), and to elucidate novel mechanisms by which cancer cells exploit neuropeptides.

Methods and analysis We analysed 180 patient samples using multiplex immunohistochemistry to assess CGRP and RAMP1 expression in primary colorectal cancer (CRC), CRC liver metastases and gastric cancers (GC). RAMP1 expression was correlated with patient demographics (age and gender) and tumour characteristics, including pathological features and molecular and genomic subtypes. RAMP1 expression and association with patient survival were evaluated using data from the Cancer Genome Atlas. The function of CGRP on tumour cell lines and patient-derived tumour organoids was assessed via in vitro stimulation assays and RNA sequencing.

Results RAMP1 expression in tumours was significantly associated with reduced survival in both CRC and GC. Over 50% of CRC and 60% of GC cells from patient samples expressed RAMP1. RAMP1 expression was enriched in tumours with microsatellite instability (MSI) and in patients with GC younger than 50 years. CGRP was abundantly expressed in stromal regions indicative of nerve fibres near tumour cells, and unexpectedly, CGRP was also produced by CRC and GC cells. Finally, CGRP stimulation enhanced tumour cell growth in a RAMP1-dependent manner, inducing genes linked to proliferation, metabolism and migration.

Conclusion This study reveals novel mechanisms by which the neuropeptide CGRP promotes tumour growth in GI cancers. We expand upon existing knowledge by demonstrating that tumour cells are a source of CGRP, highlighting potential therapeutic targets within the tumour–nerve axis.

WHAT IS ALREADY KNOWN ON THIS TOPIC

⇒ Chemical or surgical denervation of gastric nerves has been shown to reduce gastric cancer (GC) growth in humans. Recent studies demonstrate that gastric sensory nerves densely innervate GC tissues, and treatment with calcitonin gene-related peptide (CGRP) inhibitors in mouse models suppresses tumour growth.

WHAT THIS STUDY ADDS

⇒ The expression and function of CGRP and its receptor subunit receptor activity-modifying protein 1 (RAMP1) in human gastrointestinal (GI) cancers remain poorly understood. This study reveals that both CGRP and RAMP1 are expressed by tumour cells in colorectal cancer (CRC) and GC. CGRP potently stimulates tumour cell growth in a RAMP1-dependent manner, identifying the CGRP–RAMP1 axis as a novel and targetable signalling pathway in GI cancers.

HOW THIS STUDY MIGHT AFFECT RESEARCH, PRACTICE OR POLICY

⇒ These findings support the potential repurposing of existing CGRP antagonists as therapeutic agents in CRC and GC. Targeting the CGRP–RAMP1 axis may reduce tumour growth and improve patient outcomes, warranting further clinical investigation.

INTRODUCTION

Gastrointestinal (GI) cancers are a major global health burden, accounting for approximately 3.5 million deaths annually.¹ Developing effective targeted treatments for GI cancers is challenging, given the genetic and epigenetic heterogeneity of tumour cells and the complexity conferred by the broader GI tumour microenvironment (TME).² Despite this, recent advances in targeting components of the mitogen-activated protein kinase (MAPK) pathway in tumour cells, blood vessels or immune cells in the TME are improving patient outcomes.³ In addition,

there are many other components of the TME that could be explored for further benefit. Nociceptors have been found to highly infiltrate the TME, and mounting evidence suggests that tumour cells exploit the presence of nerves to promote tumour progression and metastasis.^{4–6} The GI tract is home to a rich neural network and includes the enteric nervous system (often referred to as the ‘second brain’), which, together with gut-extrinsic sensory, sympathetic and parasympathetic neurons, coordinates gut motility, secretion and blood flow for efficient digestion.⁷ The impact of crosstalk between tumour cells and neuronal factors on GI tumour progression and associated molecular mechanisms is a rapidly growing field, revealing promising new avenues for therapeutic intervention.^{8,9}

Calcitonin gene-related peptide (CGRP) is a nociceptive neuropeptide predominantly expressed by neurons of the central and peripheral nervous systems. CGRP is heavily implicated in migraine pathogenesis, and many CGRP antagonists, including the non-peptide antagonists ‘gepants’ and monoclonal antibodies, have recently been approved to treat this condition.^{10,11} This makes the translatability of these antagonists highly lucrative in their potential for treating other diseases, including cancer. CGRP⁺ nerves extensively innervate both the normal GI epithelium and GI tumours.^{6,12,13} The canonical receptor complex for CGRP is composed of functional subunits calcitonin receptor-like receptor (CALCRL) and receptor activity-modifying protein 1 (RAMP1).^{9,10,14,15} Despite the abundance of CGRP⁺ nerve fibres and high expression of RAMP1 in the GI tract,⁹ there are only a handful of studies investigating the expression and function of the CGRP–RAMP1 axis in GI cancers.⁶ Previous studies have shown that chemical or surgical denervation of gastric nerves reduces gastric tumour growth.¹⁶ Additionally, Zhi *et al* recently showed that gastric sensory nerves highly interact with gastric cancer (GC) spheroids, promoting tumour growth.⁶ In addition, analysis of GC cells in mouse gastric orthotopic tumours revealed that all innervating neurons were CGRP⁺, suggesting that CGRP is eminently involved in GC tumour progression.⁶ They also showed that CGRP⁺ nerve fibres densely innervated both human and mouse GCs.⁶ Less is known about the role of the CGRP–RAMP1 axis in colorectal cancer (CRC). Previous reports found increased CGRP in the serum of patients with CRC.^{17,18} In addition, chromogenic immunohistochemistry (IHC) revealed that both CGRP and CALCRL were highly expressed in CRC tissues.^{17,18}

Little is known about the expression of CGRP receptors, including RAMP1, in human GI cancers and how signalling via RAMP1 impacts GI tumour growth. This information is a critical missing link, necessary for informing the design of alternate cancer treatments and shedding light on the role of RAMP1 in the TME. Here, we used high-resolution multiplex IHC, RNA sequencing (RNA-seq) and model systems to directly interrogate the expression of RAMP1 and its function in collaboration with CGRP in human CRC and GC. Collectively, our results indicate

that RAMP1 is highly expressed in human CRC and GC tumour cells and that CGRP potently stimulates tumour cell growth, therefore identifying the CGRP–RAMP1 axis as a potential new target for the treatment of GI cancers.

RESULTS

RAMP1 expression in human CRC and GC is associated with poor patient outcomes

To begin to investigate the function of RAMP1 in CRC progression, we used the Cancer Genome Atlas (TCGA) data and Kaplan-Meier plotter OncoLnc¹⁹ to examine the association of *RAMP1* and *CALCRL* expression and patient prognosis. Higher expression of *RAMP1* ($p=0.0089$) was associated with decreased overall patient survival (figure 1A). There was no significant correlation between patient overall survival and expression of *CALCRL* ($p=0.8390$; figure 1B). To further investigate *RAMP1* and *CALCRL* expression across the molecular and clinical subtypes of CRC, TCGA transcriptomic data sets were further interrogated. Notably, we found that *RAMP1* was highly expressed in CRCs with microsatellite instability (MSI) compared with other molecular subtypes (chromosomally unstable (CIN) and genomically stable (GS); figure 1C). Further subdividing each stage by molecular subtype also revealed higher *RAMP1* expression in MSI compared with CIN and GS CRCs (online supplemental figure 1A). As MSI tumours are known to harbour higher immune infiltrates and immune cells are known to express RAMP1, we used CRC cell lines to investigate whether RAMP1 is expressed directly by MSI tumour cells. Consistent with the observation in primary CRCs, higher expression of *RAMP1* was also observed in MSI cell lines compared with microsatellite stable cell lines (online supplemental figure 1B). These results suggest the increase in RAMP1 expression observed in MSI CRCs is likely driven by increased RAMP1 expression in tumour cells. Comparatively, no significant trends were observed between *RAMP1* and *CALCRL* expression and tumour stage (figure 1D) or between the expression of *CALCRL* and molecular subtype and stage (figure 1E,F).

We next interrogated the expression of RAMP1 in GC, another cancer of the human GI tract. Interestingly, previous studies have found that cholinergic signalling via the vagus nerve promotes mouse GC growth,¹⁶ and Zhi *et al* recently showed that gastric sensory nerves interact extensively with mouse GC spheroids.⁶ Most GCs are adenocarcinomas (hereon referred to as GCs)²⁰; therefore, we investigated the association of *RAMP1* and *CALCRL* expression and prognosis of patients with GC. Using TCGA data and the Kaplan-Meier plotter OncoLnc, we observed that high expression of both *RAMP1* ($p=0.0127$; figure 1G) and *CALCRL* ($p=0.0477$; figure 1H) was associated with reduced overall survival in GC. Further analysis revealed that both *RAMP1* and *CALCRL* were most highly expressed in GS GCs compared with CIN, Epstein-Barr virus and MSI molecular subtypes of GC (figure 1I,K). No significant difference was observed in *RAMP1* expression

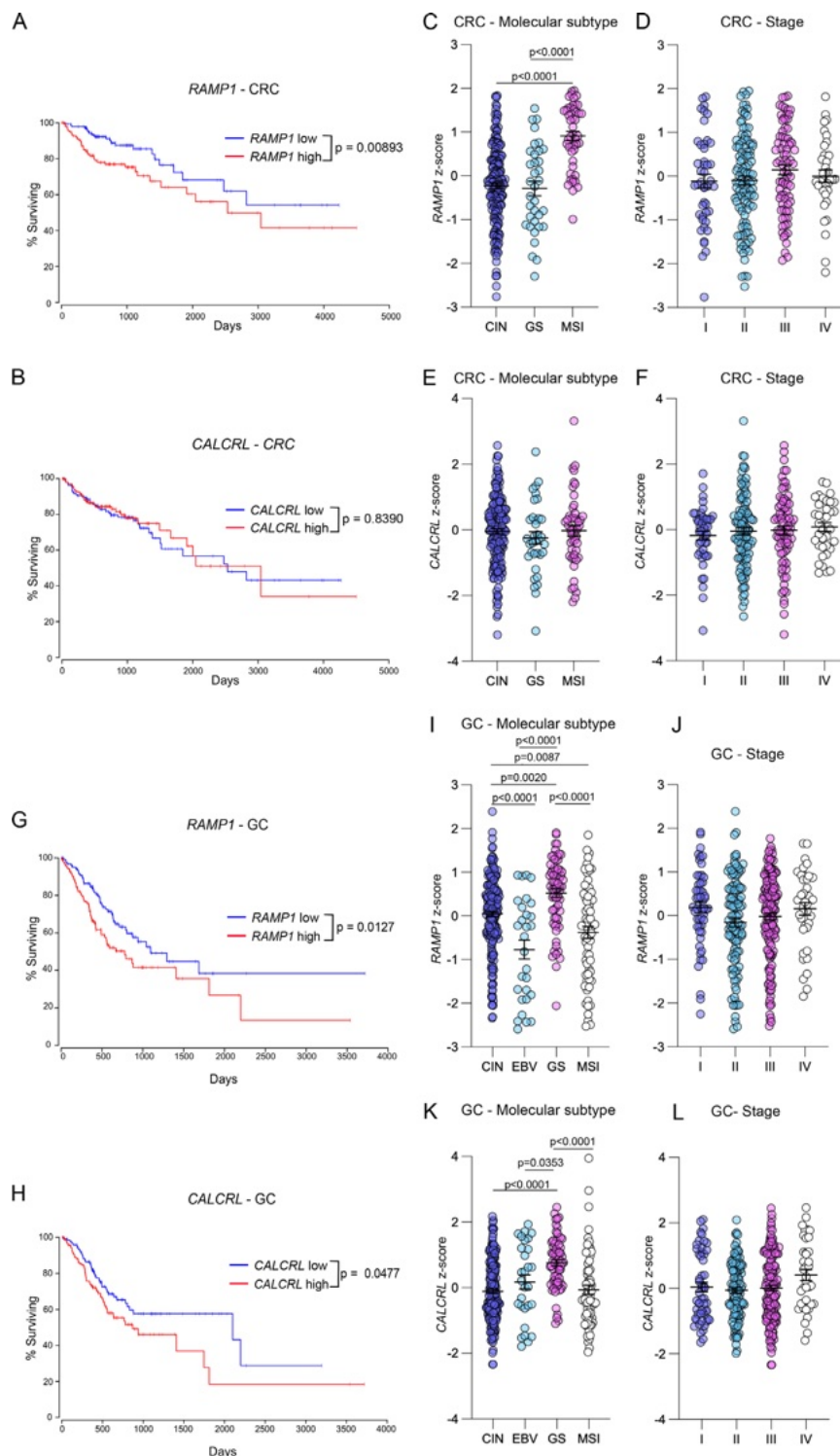


Figure 1 RAMP1 expression correlates with poor patient prognosis in CRC and GC. Analysis of TCGA tumour transcriptomic data showing overall survival of high versus low expression of (A) RAMP1 and (B) CALCRL in CRC. RAMP1 gene expression z-scores are shown for (C) CRC molecular subtype (CIN, GS and MSI) and (D) CRC disease stage. CALCRL gene expression z-scores are displayed for each (E) CRC molecular subtype and (F) CRC disease stage. Analysis of TCGA transcriptomic data showing overall survival of high versus low expression of (G) RAMP1 and (H) CALCRL in GC. RAMP1 gene expression z-scores are displayed for (I) each GC molecular subtype (CIN, EBV, GS and MSI) and (J) GC disease stage. CALCRL gene expression z-scores are displayed for each (K) GC molecular subtype and (L) GC disease stage. Groups were compared using one-way analysis of variance. The upper one-third and lower one-third percentile values were assigned for patient cohort cut-off values (CRC: $n=145$ and GC: $n=125$) for each survival analysis, and groups were compared using multivariate Cox regression analysis using OncoLnc. CALCRL, calcitonin receptor-like receptor; CIN, chromosomally unstable; CRC, colorectal cancer; EBV, Epstein-Barr virus; GC, gastric cancer; GS, genomically stable; MSI, microsatellite unstable; RAMP1, receptor activity-modifying protein 1; TCGA, the Cancer Genome Atlas.

when analysing histological subtypes as deemed by Lauren's classification (online supplemental figure 1C).²¹ However, *CALCRL* expression was upregulated in the diffuse (D) compared with the intestinal (I) histological subtype (online supplemental figure 1D). Finally, *RAMP1* and *CALCRL* expression did not differ between the GC stage (figure 1J,L). In summary, this data indicates that high expression of RAMP1 is associated with poor patient prognosis in both CRC and GC.

RAMP1 is expressed by tumour cells in primary and metastatic CRC (mCRC)

The Human Protein Atlas and the Consensus dataset²² revealed that RAMP1 was highly expressed in normal tissue from the human female reproductive tract (online supplemental figure 2A). We used healthy human cervix tissue as a positive control to test and validate an anti-human RAMP1 antibody for IHC (online supplemental figure 2B). Staining for RAMP1 revealed high expression in the human cervix, whereas there was little to no staining in human testes (negative control; online supplemental figure 2C), indicating the antibody's specificity and reliability to be used for IHC.

To investigate protein expression of RAMP1 in GI cancers, we used formalin-fixed paraffin-embedded (FFPE) CRC tissue microarrays (TMAs). TMAs were stained with anti-RAMP1 (yellow) and for Pan-cytokeratin (PanCK) or cytokeratin (red). Samples were counterstained with 4',6'-diamidino-2-phenylindole (DAPI) (blue) to recognise cell nuclei. Staining of stage II and stage III primary CRCs and liver mCRC revealed that RAMP1 was highly and specifically expressed on cytokeratin-positive tumour cells (figure 2A). Quantification of the percentage of RAMP1-expressing tumour cells in each sample revealed that, on average, over 50% of tumour cells in stage II and stage III CRCs, as well as mCRCs, stained positive for RAMP1 (figure 2B). We were surprised to observe such a high frequency of RAMP1-expressing tumour cells in CRC, and therefore, we further confirmed expression of RAMP1 using in situ hybridisation (RNAscope; online supplemental figure 2D). We observed a punctate staining pattern representing *RAMP1* messenger RNA that co-localised with cytokeratin-expressing tumour cells. Consistent with our IHC staining, we observed low levels of *RAMP1* staining in the tumour stroma (online supplemental figure 2D). In summary, these experiments show that RAMP1 is highly expressed by tumour cells in primary CRC and mCRC.

Assessment of additional tumour characteristics, including age, gender, grade, tumour stage, tumour location, invasive front, venous invasion, mucinous differentiation and Crohn's-like lymphoid reaction score (figure 2C,D and online supplemental figure 3A–F), revealed that RAMP1 was most significantly expressed in tumours originating in the proximal and distal colon compared with the rectum (figure 2C). We also investigated the association of RAMP1 expression with common genetic drivers of CRC, including BRAF and TP53²³;

however, no association with RAMP1 expression was observed (online supplemental figure 3G,H).

Overall, our analysis of RAMP1 expression in CRC highlights a potential role for RAMP1 in controlling the growth of human CRC cells, especially in tumours arising in the proximal and distal colon relative to the rectum.

CGRP enhances tumour cell growth in CRC

To directly investigate the function of CGRP and RAMP1 on tumour cell growth in CRC, we stimulated the human CRC cell line HT115, which expresses both *RAMP1* and *CALCRL*²⁴ (figure 2E). Stimulation of HT115 cells with a range of CGRP concentrations (from 10^{-6} M to 10^{-9} M) enhanced the number of tumour cells compared with unstimulated cells (figure 2F). In addition, deletion of RAMP1 using CRISPR/Cas9 in HT115 cells significantly reduced tumour cell growth in both unstimulated and CGRP-stimulated cells compared with HT115 wild-type cells. We also used a colorimetric 3-(4,5-dimethylthiazol-2-yl)-5-(3-carboxymethoxyphenyl)-2-(4-sulfophenyl)-2H-tetrazolium (MTS) assay to measure cell proliferation and found that stimulation of HT115 cells with CGRP resulted in a significant, concentration-dependent increase in tumour cell growth (online supplemental figure 3I). These results establish RAMP1 as a critical factor required for HT115 cell growth and proliferation at steady state and following CGRP stimulation.

To further investigate the function of CGRP on tumour cell growth, we used patient-derived tumour organoids (PDTOs). Following stimulation with CGRP (10^{-7} M and 10^{-6} M) for 7 days, we observed a significant increase in organoid size from two independent PDTOs (figure 2G,H). Together, these findings demonstrate that CGRP signalling promotes CRC growth in vitro and highlight both CGRP and RAMP1 as potential therapeutic targets in CRC.

RAMP1 is highly expressed by GC cells in younger individuals

CGRP⁺ nerve fibres were recently discovered to be highly expressed in GC and shown to promote tumour growth.⁶ However, further research is required to fully appreciate the distribution of CGRP co-receptor RAMP1, its expression and function in human GC. Therefore, we performed multiplex IHC on GC TMAs and stained for RAMP1 and PanCK to identify tumour cells (figure 3A). We also stained an additional cohort of gastro-oesophageal junction (GOJ) tumours, which closely align with the CIN molecular subtype and Lauren's intestinal classification of GC.^{25,26} We observed co-localisation of RAMP1 and cytokeratin staining across each subtype of GC. This analysis revealed that RAMP1 was highly and specifically expressed on cytokeratin-expressing tumour cells (figure 3A). On average, over 70% of tumour cells in diffuse GCs and over 60% of tumour cells across intestinal- and GOJ-GC expressed RAMP1 (figure 3B). Assessment of patient characteristics, including age, revealed that RAMP1

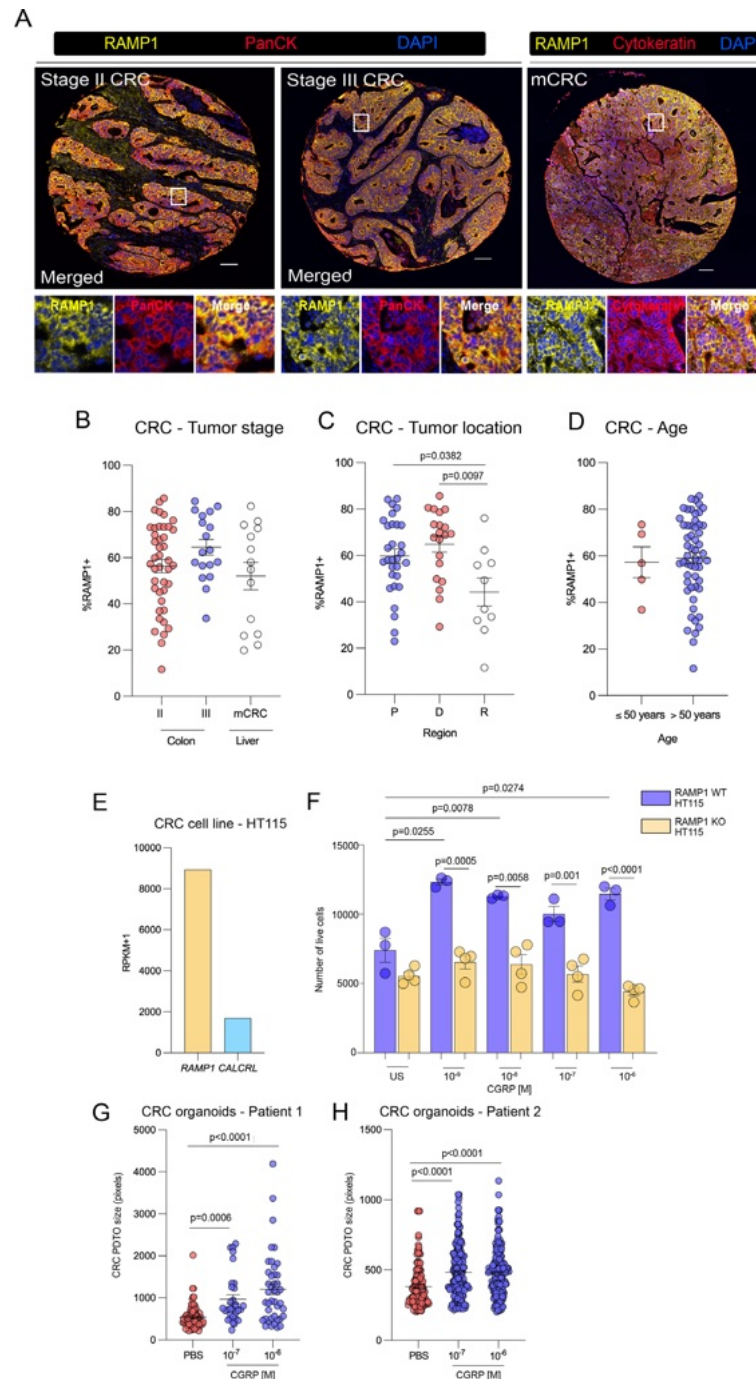


Figure 2 RAMP1 is highly expressed in primary and mCRC, and CGRP promotes tumour cell growth. (A) Representative IHC staining of RAMP1 (yellow), PanCK (red)/cytokeratin (red) and DAPI (blue) in stage II and stage III CRC and liver mCRC. (B) Quantitative analysis of IHC staining showing frequency of RAMP-expressing tumour cells according to CRC tumour stage. Frequency of RAMP1-expressing tumour cells for stage II and III patients according to (C) tumour location and (D) patient age. Each data point represents the frequency of RAMP1-expressing tumour cells for one patient tumour, averaged from at least two replicate tissue microarray cores. Scale bars=100 μ m. (E) Expression of *RAMP1* and *CALCRL* in HT115 human CRC cells. (F) Number of live cells at day 7 following control (US) or CGRP stimulation of WT or *RAMP1* KO HT115 cells. CGRP stimulation concentrations ranged from 10^{-6} to 10^{-9} as indicated. Each data point represents the average of three technical replicates and is the pooled data of 3–4 independent experiments. Error bars represent mean \pm SEM, with p values calculated using Welch's t-test. CRC organoids derived from two independent patients, (G) patient 1 and (H) patient 2, were stimulated with control PBS or CGRP at the indicated concentrations for 7 days. Each data point represents the size of an individual patient-derived tumour organoid identified in the assay well. Error bars represent mean \pm SEM, with groups compared using one-way analysis of variance. *CALCRL*, calcitonin receptor-like receptor; CGRP, calcitonin gene-related peptide; CRC, colorectal cancer; DAPI, 4',6'-diamidino-2-phenylindole; GC, gastric cancer; GOJ, gastro-oesophageal junction; IHC, immunohistochemistry; KO, knockout; mCRC, metastatic CRC; PanCK, Pan-cytokeratin; PBS, phosphate-buffered saline; RAMP1, receptor activity-modifying protein 1; US, unstimulated; WT, wild-type.

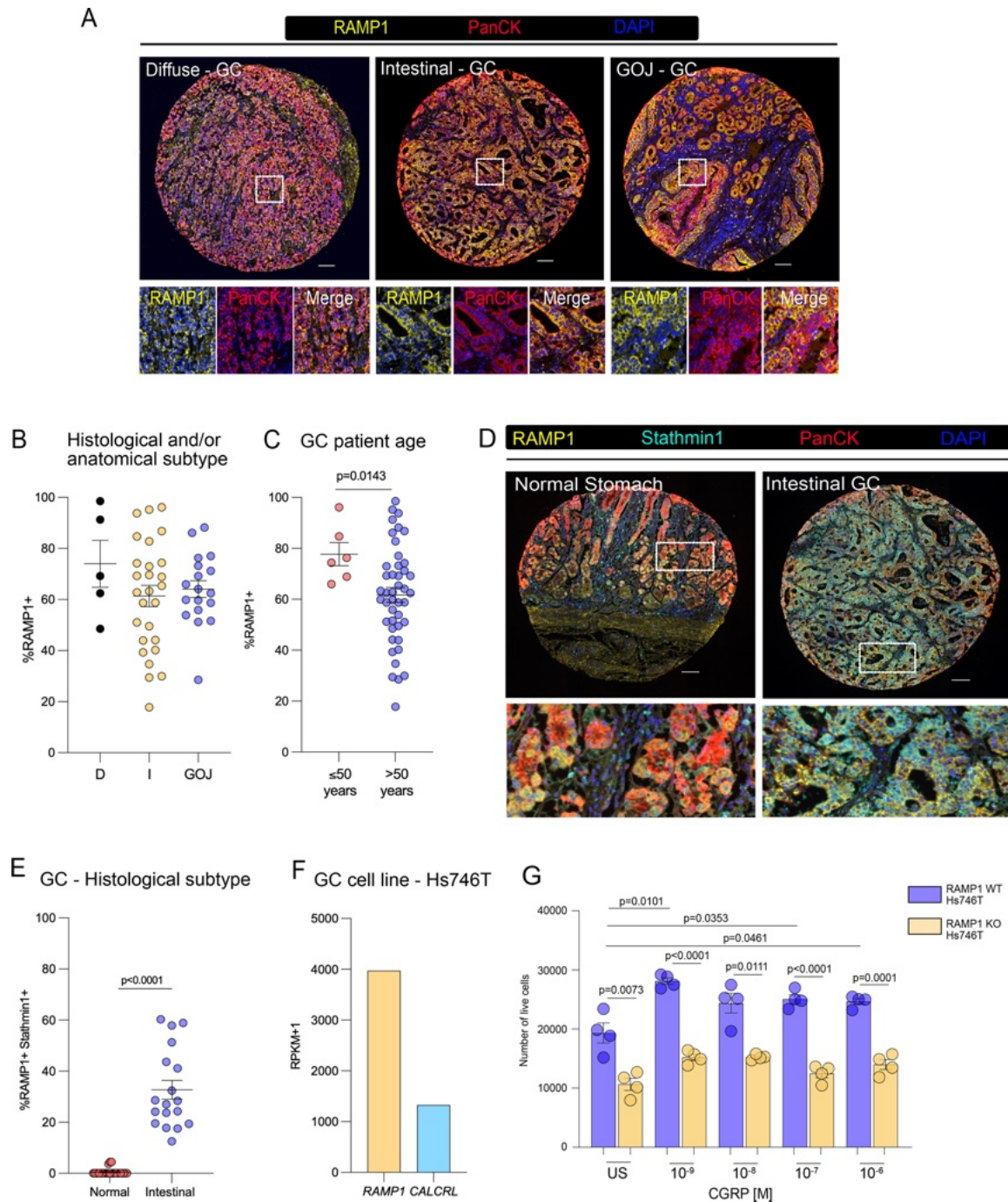


Figure 3 RAMP1 is highly expressed in human GC, and CGRP promotes the growth of human GC cell lines in vitro. (A) Representative IHC staining of RAMP1 (yellow), PanCK (red) and DAPI (blue) in diffuse and intestinal type GCs and GCs from the GOJ. (B–C) Quantitative analysis of IHC staining showing the frequency of RAMP1-expressing tumour cells in GC according to (B) histological and/or anatomical subtypes and (C) patient age. Each data point is indicative of one patient's tumour, with data averaged from at least two separate TMA cores. (D) Representative IHC staining of RAMP1 (yellow), Stathmin1 (cyan), PanCK (red) and DAPI (blue) of healthy stomach and the intestinal subtype of GC. (E) Quantitative analysis of healthy stomach and intestinal GC cells expressing both RAMP1 and Stathmin1. The frequency of RAMP1 Stathmin1 tumour cells is shown. Each data point is indicative of one patient's tumour, which is averaged from at least two separate TMA cores. Scale bars=100 μ m. Error bars represent mean \pm SEM, and groups were compared using Welch's t-test. (F) Expression of *RAMP1* and *CALCRL* in the Hs746T human GC cell line. (G) Number of live cells at day 5 following control (US or CGRP stimulation of WT or *RAMP1* KO Hs746T cells. CGRP stimulation concentrations ranged from 10^{-6} to 10^{-9} as indicated. Each data point represents the average of three technical replicates and is the pooled data of four independent experiments. Error bars represent mean \pm SEM, with p values calculated using Welch's t-test. *CALCRL*, calcitonin receptor-like receptor; *CGRP*, calcitonin gene-related peptide; *CRC*, colorectal cancer; *DAPI*, 4',6'-diamidino-2-phenylindole; *GC*, gastric cancer; *GOJ*, gastro-oesophageal junction; *IHC*, immunohistochemistry; *KO*, knockout; *mCRC*, metastatic *CRC*; *PanCK*, Pan-cytokeratin; *RAMP1*, receptor activity-modifying protein 1; *TMA*, tissue microarray; *US*, unstimulated; *WT*, wild-type.

was significantly more highly expressed on tumour cells in patients known drivers of tumours with GC aged 50 years and below (figure 3C). There was no association of RAMP1 staining and the extent of perineural invasion, lymphovascular invasion, venous invasion or tumour stage (online supplemental figure 4A–D). GC is driven by genetic mutations in known drivers of tumorigenesis, including TP53, while overexpression of the transcription factor CDX2 is associated with the development of intestinal-type GCs.^{25 27 28} However, no association between RAMP1 expression and TP53 expression or CDX2 expression were observed (online supplemental figure 4E,F).

We next stained a cohort of healthy stomach tissue and intestinal GCs with Stathmin1 and RAMP1. Stathmin1 is a marker of cell proliferation and an oncoprotein, which has a crucial role in spindle assembly and disassembly during mitosis and is highly expressed in multiple cancers.²⁹ GCs and healthy stomach samples were stained with RAMP1 (yellow), Stathmin1 (cyan), PanCK (red) and DAPI (blue) (figure 3D). The proportion of PanCK-expressing epithelial or tumour cells that stained for both RAMP1 and Stathmin1 was significantly higher in intestinal GC compared with healthy stomach (figure 3E). In summary, these experiments show that RAMP1 is highly expressed by cells expressing the proliferative marker Stathmin1 in GC, and RAMP1 is highly expressed in GC, especially in younger individuals.

CGRP enhances GC cell growth

To investigate the function of RAMP1 and its co-receptor CALCRL in GC cell growth, we investigated the effect of CGRP stimulation on cell proliferation of two human GC cell lines, Hs746T²⁴ (figure 3F). Stimulation of Hs746T cells with CGRP led to a significant increase in tumour cell growth as determined 5 days after stimulation by flow cytometry (figure 3G) and the MTS assay (online supplemental figure 4G). In contrast, stimulation of SNU601 GC cells, which expressed low levels of RAMP1 and CALCRL (online supplemental figure 4H), exhibited a modest increase in cell proliferation (online supplemental figure 4I). Furthermore, CRISPR/Cas9 deletion of RAMP1 in Hs746T GC cells led to a significant decrease in cell number following culture for 5 days and in response to CGRP stimulation. Together, these results show that CGRP and RAMP1 play an important role in promoting the growth of GC cells.

CGRP is produced by tumour cells in CRC and GC

To assess CGRP expression and spatial distribution in the progression of CRC and GC, we next stained a small cohort of CRC and GC samples containing tumour and normal surrounding tissue (figure 4). CGRP⁺ staining appeared as granular or punctate and, as expected, was observed in thin, branched structures potentially representing nerve fibres in the stromal regions of normal and tumour tissue (figure 4A,D). Surprisingly, we also observed CGRP co-staining on PanCK⁺ tumour cells in

both CRC and GC samples (figure 4A,D). Additional representative images where we co-stained for CGRP, RAMP1 and PanCK revealed RAMP1⁺ tumour cells in close proximity to CGRP⁺ tumour and stromal cells (online supplemental figure 5A,B). Analysis of CRC samples revealed that total CGRP staining was significantly elevated in stage III CRC compared with stage II and mCRC (figure 4B). Interestingly, when CGRP staining was stratified by PanCK⁺ (tumour or epithelial) and stromal regions, we observed a significant increase in CGRP expressed by PanCK⁺ tumour cells, particularly in stage III CRC (figure 4C).

We observed a similar trend in GC, with a significant increase in total CGRP⁺ expression in intestinal-type GC compared with normal stomach, diffuse and GOJ tumours (figure 4E). Notably, CGRP staining was significantly higher in PanCK⁺ tumour cells of intestinal-type GC relative to GOJ tumours and was also elevated in PanCK⁻ stromal regions compared with both diffuse and GOJ tumours (figure 4F).

To verify that CGRP is produced by tumour cells, we further examined the cell lines used in this study for CALCA (the gene encoding α CGRP) expression. Consistent with the expression of CGRP in PanCK⁺ tumour cells in CRC and GC, we also observed CALCA expression in the HT115 and Hs764T cell lines (online supplemental figure 5C).

CGRP promotes gene pathways associated with tumour proliferation and metastasis

To understand the gene pathways induced by CGRP that enhance tumour cell growth, we performed RNA-seq to identify differentially expressed genes (DEGs) after CGRP stimulation of Hs746T human GC cells (figure 5A,B). Stimulation with CGRP for 2 days induced gene expression changes, with numerous genes increased in expression (figure 5A). The induced genes included genes associated with angiogenesis, cell metabolism, adhesion, migration and invasion. Specifically, proangiogenic factor vascular endothelial growth factor-A (VEGFA), while Procollagen-Lysine,2-Oxoglutarate 5-Dioxygenase 2 (PLOD2), which is known to modify the TME by inducing production of collagen, was also increased in expression³⁰ (figure 5B). Notably, PLOD2 was recently shown to promote the proliferation and invasion of CRC tumour cells.³¹ We also observed increases in several genes previously shown to enhance cancer cell growth (BNIP3, ETNK1, PDK1, PDK3 and PFKL).^{32–38} In addition, we observed enhanced expression of several genes involved in apoptosis or ferroptosis (MIR210HG and BHLHE40)^{39 40} (figure 5B). The DEGs were interrogated in the Metascape portal, which provides automated analyses of genes into common biological, gene ontology pathways and protein networks.⁴¹ Wound repair and MAPK signalling pathways were both downregulated, while hypoxia and peptidyl-amino acid modification pathways were upregulated. These findings reveal potential new mechanisms

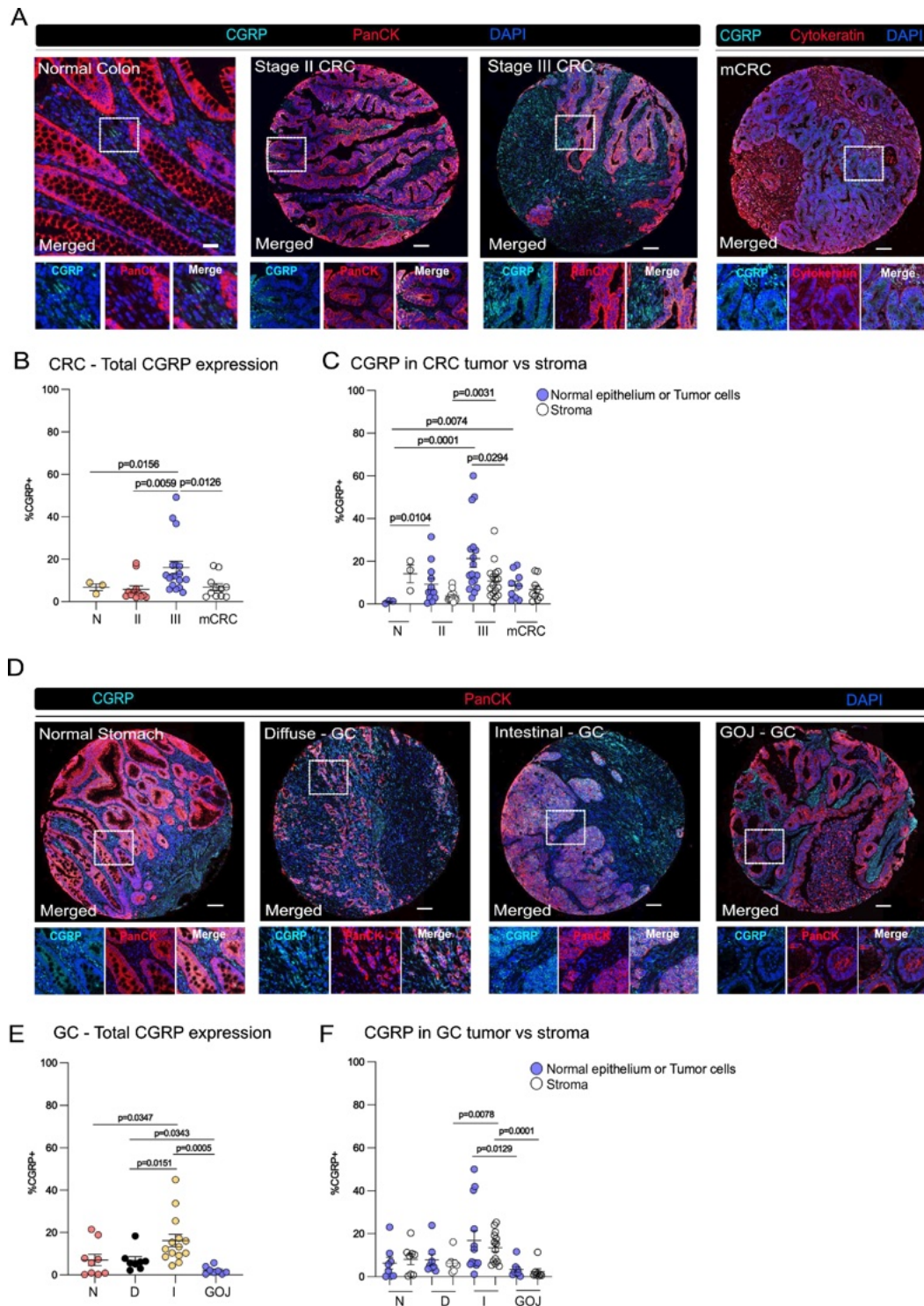


Figure 4 CGRP is produced by tumour cells in CRC and GC. (A) Representative immunohistochemistry staining of CGRP (cyan), PanCK (red)/cytokeratin (red) and DAPI (blue) in normal tumour-adjacent colon (N), stage II and stage III CRC and liver mCRC. (B) Quantitation of (A) showing frequency of CGRP-expressing cells among total cells for each normal or tumour sample. (C) Quantitation of (A) showing frequency of CGRP-expressing cells from stromal versus epithelial cells in each normal tumour-adjacent colon or CRC sample. (D) Representative immunohistochemical staining of CGRP (cyan), PanCK (red) and DAPI (blue) in N, D and I type GCs, and GCs from the GOJ. (E) Quantitation of (D) showing frequency of total CGRP-expressing cells in each normal tumour-adjacent stomach sample or GC sample. (F) Quantitation of (D) showing frequency of CGRP-expressing stromal versus epithelial cells in each normal stomach or GC sample. Each data point represents one patient sample averaged from two to three different tissue areas of the same sample. Scale bars=100 μ m for all images except for (A) normal tumour-adjacent colon, which is 30 μ m. Error bars represent mean \pm SEM, with groups compared using Welch's t-test. CGRP, calcitonin gene-related peptide; CRC, colorectal cancer; D, diffuse; DAPI, 4',6'-diamidino-2-phenylindole; GC, gastric cancer; GOJ, gastro-oesophageal junction; mCRC, I, intestinal; mCRC, metastatic CRC; N, normal stomach; PanCK, Pan-cytokeratin.

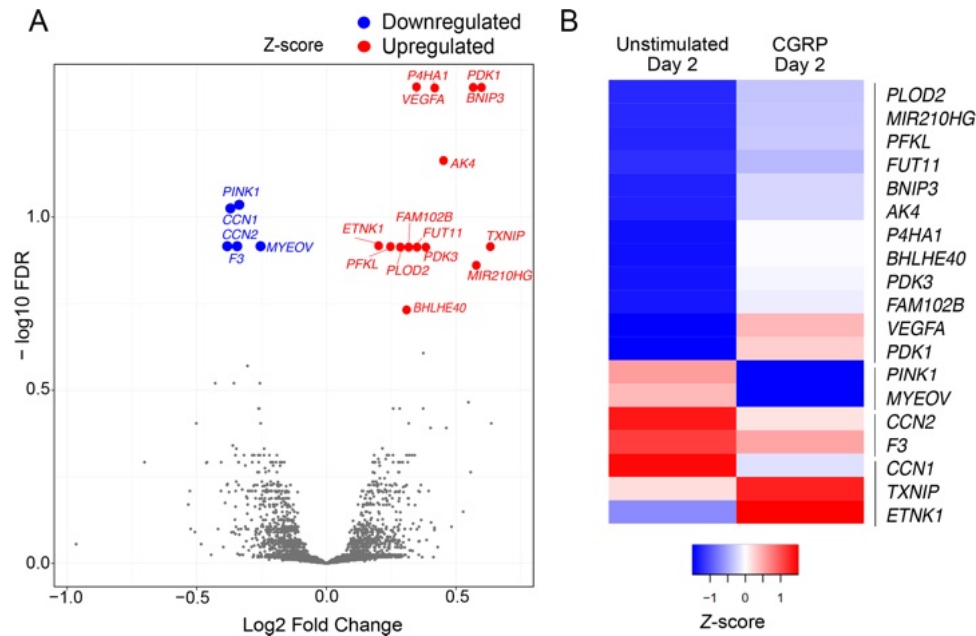


Figure 5 CGRP promotes GC gene expression associated with tumour cell proliferation and metastasis. RNA sequencing of cultured human Hs746T GC cells stimulated with or without 10^{-6} M CGRP for 2 days. (A) Volcano plot and (B) heatmap displaying differentially expressed genes (false discovery rate cut-off of 0.2). CGRP, calcitonin gene-related peptide; FDR, false discovery rate; GC, gastric cancer.

by which CGRP may promote tumour cell growth in GI cancers.

DISCUSSION

Recent studies report high nerve fibre densities, notably nociceptors, within human tumours, where they have been proposed to interact with cancer cells, immune cells, fibroblasts and other cells of the TME to promote tumour growth and metastasis.^{5 6 16 42 43} The sensory neuropeptide CGRP has recently attracted significant interest due to its expression and function in promoting tumorigenesis in mouse models of GC.⁶ However, more research is needed to fully elucidate the role of CGRP and its receptor subunit, RAMP1, in human GI cancers. The availability of highly specific and validated antibodies to investigate RAMP1 within the human TME has been a major limitation. Here, we used both anti-RAMP1 and anti-CGRP antibodies and RNA in situ hybridisation probes in imaging experiments to investigate the expression and spatial distribution of RAMP1 and CGRP in human CRC and GC. We found that RAMP1 and CGRP are both highly expressed by primary tumour cells in human CRC and GC. In addition, we observed robust staining of RAMP1 and CGRP in mCRC lesions isolated from liver resections.

The risk of developing GI cancers over the age of 50 is higher; however, there has been a recent uprise in both GC and CRC being diagnosed in younger adults.⁴⁴ Interestingly, we observed a significant increase in RAMP1 expression in patients with GC younger than 50 years. Further research is needed to reveal the factors involved in regulating CGRP and RAMP1 expression in the steady-state stomach, colon and in tumour settings. Recent

reports show that distinct epithelial cell types express RAMP1 in the healthy stomach and colon.^{6 9} RAMP1 is expressed predominantly by endocrine cells in the normal human stomach⁶ and by mucus-producing goblet cells in the normal colon.⁹ Therefore, distinct factors are likely involved in regulating the expression of RAMP1 in the colon versus the stomach. Nevertheless, RAMP1 was associated with poor patient prognosis in both CRC and GC. CGRP is predominantly expressed by sensory neurons in the GI tract; however, it can also be produced by other cell types, including group 2 innate lymphoid cells, which also increase in GI cancers.^{15 45–48} Importantly, future studies will be necessary to fully elucidate factors controlling CGRP release by tumour cells and the broader implications for the TME. Our findings reveal that CGRP potentially promotes the growth of both RAMP1-expressing GC and CRC cells in vitro. Together, these results suggest that CGRP signals via RAMP1 and play a significant role in controlling the growth of human CRC and GC.

Our results reveal several mechanisms by which CGRP and RAMP1 signalling may enhance tumour growth. These include cell-intrinsic mechanisms, where CGRP stimulation of human GC cells significantly increased the expression of genes associated with cell proliferation and metabolism. We also observed potential tumour cell-extrinsic functions of CGRP that could impact the TME. Specifically, CGRP enhanced the expression of *PLOD2* and *VEGFA*, which are important for collagen production and blood vessel formation, respectively, in rapidly growing tumours, thereby improving oxygen delivery to fuel cancer growth.^{30 31 36} Recent reports have also shown

that CGRP can act on immune cells within the TME. For instance, CGRP has been found to promote CD8⁺ T cell exhaustion, reducing T cell activity and limiting anti-tumour immune responses.^{5, 49} In light of our findings, we hypothesise that blocking CGRP–RAMP1 signalling in human GI tumours would directly limit tumour cell growth and modify the TME while also enhancing CD8⁺ T cell immunity, ultimately reducing cancer progression and improving patient survival.

There are several methods used to target nerves therapeutically, including denervation, treatment with neuronal receptor antagonists and inhibitors of neuroendocrine factors.⁴ Although denervation has shown promise in GC mouse models¹⁶ and in a phase 2 clinical trial (NCT01822210)⁴, its efficacy in metastatic GC has been difficult to validate.¹⁶ There have also been side effects, including the growth of cancer-related lesions after denervation in rats.⁵⁰ β -blockers (including propranolol and propranolol hydrochloride), which target adrenergic nerves, are being used alongside immunotherapy in a number of clinical trials in a range of cancers, including CRC (NCT03919461) and GC (NCT03245554).⁴ Recently, Zhi *et al* used the non-peptide antagonist of CGRP, rimegepant, to reduce GC growth both in mouse models in vivo and in vitro.⁶ Therefore, targeting nerves via such antagonists is an area of research with great potential in cancer medicine; however, more research is needed to fully elucidate the mechanisms and potential of therapeutically targeting RAMP1 in GI cancers, particularly in humans. Monoclonal antibodies (mAbs) are heavily exploited in cancer treatment. There are four mAbs (erenumab, galcanezumab, eptinezumab and fremanezumab) which potently antagonise the CGRP–RAMP1 axis and are very successful in reducing episodic and chronic migraine frequency.⁵¹ Future research exploiting these clinically available tools could show promise in targeting RAMP1 receptors expressed by GI tumour cells and different compartments of the TME, including CD8⁺ T cells. Therefore, our work showing that RAMP1 is a key player in the tumour cell–neuronal axis has the potential to unlock innovative treatment approaches to benefit patients with GI in the future.

METHODS

Study participants

CRC stage II–IV primary tumour samples, liver metastasis (n=106), normal colon (n=3) or GC stage I–IV samples (n=71) from both male and female donors were retrospectively collected and deidentified from patients recruited at Austin Health or by the Victorian Cancer Biobank, for whom clinical data were collected. Assessment of tumour characteristics, including venous invasion, mucinous differentiation, Crohn's-like lymphoid reaction score, invasive front, BRAF mutation, TP53 expression, CDX2 expression, perineural invasion and lymphovascular invasion, has been previously described.^{52–55}

Fluorescent multiplex IHC

Human TMAs and whole tissue FFPE sections were stained with antibodies and/or RNAscope probes using the Opal 7-colour multiplex IHC kit (Akoya Biosciences). Staining was performed using the manual staining protocol according to the manufacturer's instructions. The following antibodies/probes were used: RAMP1 (ab203282, Abcam), CGRP (PA5-114929, Invitrogen), Stathmin1 (A4379, ABclonal), PanCK (PA0094-U, Leica), cytokeratin 8/18 (NCL-L-5D3, Leica), RNAscope 2.5 Probe-Hs-RAMP1-C2 (ADV483051C2, Advanced Cell Diagnostics) and DAPI. Whole slide scans at 10 \times magnification were performed using the Vectra 3 Automated Quantitative Pathology Imaging System (Akoya Biosciences) and Phenochart (Akoya Biosciences) to identify and map individual TMA cores to then obtain 20 \times magnification multispectral images for analysis. For full face tissue sections, 20 \times magnification multispectral images were obtained. A spectral library was created to unmix images and subtract autofluorescence using InForm Analysis Software (Akoya Biosciences), and cell frequencies were quantified using the HALO imaging platform (Indica Labs, Albuquerque, New Mexico, USA). At least two TMA cores from each patient were used to obtain an average value for RAMP1 or CGRP expression for analysis. Cell segmentation was performed using nuclear, membrane and cytoplasmic staining. Scale bars were added using FIJI (V.2.0.0-rc-59/1.51n).

In vitro cell proliferation assays

Cell line assays

HT115, Hs746T and SNU601 cells were grown in media (Dulbecco's modified Eagle medium/nutrient mixture F-12, Thermo Fischer, Australia), supplemented with 10% v/v foetal bovine serum (Bovogen Biological, Australia) in 175 cm² flasks (Corning, New York, USA). 5 \times 10³ cells were seeded in 96-well round-bottom plates (Corning) and stimulated with 10⁻⁶ to 10⁻⁹ M α CGRP (C0167, Merck, Australia) on day 1. α CGRP was diluted in MilliQ water according to the manufacturer's instructions. The number of viable cells was measured on day 7 for HT115 cells and day 5 for Hs746T cells. Briefly, cells were washed with phosphate-buffered saline (PBS, Thermo Fischer) and trypsinised (Thermo Fischer) before incubation with the viability marker, propidium iodide (Merck), which binds to dead cells. Cells were analysed with a BD FACS Canto II Flow Cytometer, and data were analysed using FlowJo V.10.10.0.

Cell proliferation was also measured with the CellTiter 96 AQueous One Solution Reagent kit using the tetrazolium compound MTS (inner salt, G3580, Promega, Australia) on day 5 (for Hs746T and SNU601) and day 7 (for HT115), where 20 μ L of MTS was added to each well containing 100 μ L of fresh media. Plates were incubated for at least 1 hour, and absorbance was measured using a spectrophotometer (Spectrostar Nano, BMG Labtech, Australia).

PDTO assays

CRC organoids were recovered and expanded using methods described in previous publications.⁵⁶ CRC organoids were grown for 2 weeks after recovery from liquid nitrogen. Cells were trypsinised into single-cell suspensions and plated into 384-well plates at a density of 3000 cells per well. Organoids were grown at 37°C for 3 days to grow into small organoids before treatment with PBS or CGRP. Each well of the organoid assay plates was imaged at the NIKON LIPSI live-cell image system every 24 hours for 7 days. Organoid sizes were measured by image analysis using ImageJ.

Electroporation (nucleofection) of recombinant CRISPR/Cas9 and single guide RNA (sgRNA)

RAMP1 sgRNA 5'-AGUGGUCAUGAAGAGGUGAU-3' was synthesised by IDT (Singapore). HT115 or Hs746T cells were electroporated with either a Cas9-only control or Cas9/guide RNA ribonucleoproteins using the SF Cell Line 4D-Nucleofector X kit (Lonza). Knockout efficiency was assessed by multiplex IHC.

Cell extraction and RNA purification

Hs746T cells were stimulated with 10^{-6} M α CGRP. On day 2 following stimulation, cells were trypsinised (Thermo Fischer) and lysed with lysis buffer (Buffer RLT Plus RNeasy Plus Lysis Buffer, Qiagen, Australia), 1% v/v β -mercaptoethanol (Sigma, Australia) and stored at -30°C until RNA purification. RNA was purified using the RNeasy Plus Micro Kit (Qiagen). RNA was eluted in 14 μL of RNase-free water and stored at -80°C . RNA quality was tested using a 4200 TapeStation (Agilent, Australia).

Bulk RNA-seq

100 ng of total RNA per sample was used for next-generation sequencing (NGS) library preparation (FC-122-2002, Illumina TruSeq RNA, USA) as per the manufacturer's instructions. NGS libraries were pooled and sequenced using a P2 100-cycle Illumina sequencing kit (20046811, Illumina) on the NextSeq 1000 sequencing system (Illumina) with paired-end 66 base pair reads. Sequencing reads were mapped to the GRCh38/hg38 reference genome using the Subread aligner in the Subread package (V.2.0.7).^{57 58} Multimapping reads were allowed, and gene-wise read counts were obtained using the featureCounts programme included in the Subread package.⁵⁹ Subread Inbuilt RefSeq annotation for human (build 38.1) was used in the read summarisation. Only genes that achieved at least 10 counts per million (CPM) in at least two samples were included in the downstream analysis. Genes without official symbols, pseudogenes, mitochondrial genes and ribosomal genes were excluded. Gene counts were converted to \log_2 -CPM, quantile-normalised and precision-weighted using the limma voom function.^{60 61} Normalised \log_2 -CPM expression values of genes were then converted to \log_2 -reads per kilobase per million mapped reads (RKPM) values. A linear model was fitted to each gene (using limma's

lmFit function), and an empirical Bayes moderated t-statistic was used to assess differential expression of genes.⁶² Genes were identified as differentially expressed if they achieved a false discovery rate cut-off of 0.2.

Analysis of TCGA RNA-seq data

GC (stomach adenocarcinoma) and CRC (colon adenocarcinoma) patient data from TCGA were downloaded from the University of California, Santa Cruz Xena database. This database contains gene transcription data, which has been analysed using the Illumina HiSeq2000 RNA Sequencing Platform (University of North Carolina), expressed as either RPKM or RNA-Seq by Expectation-Maximisation. Genes of interest were extracted and correlated with the appropriate clinical and molecular subtypes obtained from cBioPortal, and z-score normalised per gene row ($z = (x - \mu) / \sigma$) and plotted using GraphPad Prism (Boston, Massachusetts, USA).

Statistical analysis

All data were analysed using GraphPad Prism V.10.2.3 for MacOS (GraphPad Software). Multivariate Cox regression analysis, multiple comparisons, one-way analysis of variance and Welch's t-tests were performed to determine statistical significance. A p value of less than 0.05 was considered statistically significant.

Author affiliations

- ¹Olivia Newton-John Cancer Research Institute, Heidelberg, Victoria, Australia
- ²School of Cancer Medicine, La Trobe University, Heidelberg, Victoria, Australia
- ³La Trobe Institute for Molecular Science, La Trobe University, Bundoora, Victoria, Australia
- ⁴Personalised Oncology Division, Walter and Eliza Hall Institute of Medical Research, Melbourne, Victoria, Australia
- ⁵Department of Medical Biology, The University of Melbourne, Parkville, Victoria, Australia
- ⁶Department of Biochemistry and Molecular Biology, Biomedicine Discovery Institute, Faculty of Medicine, Nursing and Health Sciences, Monash University, Clayton, Victoria, Australia
- ⁷Department of Medicine, Alfred Hospital, School of Translational Medicine, Monash University, Melbourne, Victoria, Australia
- ⁸Department of Surgery, The University of Melbourne, Parkville, Victoria, Australia
- ⁹Department of Biochemistry and Molecular Biology, Monash University, Clayton, Victoria, Australia
- ¹⁰Department of Immunology, Harvard Medical School, Boston, Massachusetts, USA
- ¹¹Department of Anatomical Pathology, Austin Health, Heidelberg, Victoria, Australia

Acknowledgements We thank our consumers and patient advocates for their advice, patients and their families who donated human tissues for use in this study and the Austin Hospital ethics committee for their guidance. The results published here are in part based upon data generated by the TCGA Research Network: <https://www.cancer.gov/tcga>. We also thank the Victorian Cancer Biobank through the Cancer Council Victoria as Lead Agency, which is supported by the Victorian Government through the Victorian Cancer Agency, a business unit of the Department of Health.

Contributors PP: conceptualisation, data curation, formal analysis, investigation, methodology, validation, visualisation, writing the original draft, writing the review and editing and project administration. KT: investigation, methodology, visualisation, writing the review and editing. LN and TT: investigation and methodology. ALEC: data curation, formal analysis, writing the review and editing. YL: data curation, formal analysis and software. DM: investigation. JDGD: resources, writing the review and editing. AH: methodology. CJK: methodology, resources and supervision. BP: supervision and methodology. PG: resources. OMS: resources and supervision. WS: supervision, data curation, formal analysis and software. IMC: supervision.

JMM: data curation, formal analysis, resources, writing the review and editing. DSW: data curation, formal analysis, investigation, resources, writing the review and editing. MB: supervision, data curation, writing the review and editing. LAM: conceptualisation, data curation, visualisation, writing the original draft, writing the review and editing, project administration, supervision and funding acquisition. LAM is the guarantor.

Funding This work was supported by the Australian National Health and Medical Research Council Ideas Grants 2011558 (LAM) and 1185513 (LAM and DSW), Victorian Cancer Agency mid-career fellowship 1123388 (LAM), a Tour de Cure Postgraduate PhD Scholarship Grant (PP), Tour de Cure Senior Investigator Grant (LAM) and the Stafford Fox Medical Research Foundation (OMS). This publication is based on research supported by the Colorectal Cancer Alliance award 10021225.

Competing interests None declared.

Patient and public involvement Patients and/or the public were involved in the design, or conduct, or reporting, or dissemination plans of this research. Refer to the Methods section for further details.

Patient consent for publication Not applicable.

Ethics approval This study involves human participants and patient samples were approved by the Austin Health Human Research Ethics Committee (HREC/15/Austin/359 and 75462) and WEHI Human Research Ethics Committee (HREC 2016.249, WEHI). Participants gave informed consent to participate in the study before taking part.

Provenance and peer review Not commissioned; externally peer reviewed.

Data availability statement Data are available upon reasonable request. All data relevant to the study are included in the article or uploaded as supplementary information.

Supplemental material This content has been supplied by the author(s). It has not been vetted by BMJ Publishing Group Limited (BMJ) and may not have been peer-reviewed. Any opinions or recommendations discussed are solely those of the author(s) and are not endorsed by BMJ. BMJ disclaims all liability and responsibility arising from any reliance placed on the content. Where the content includes any translated material, BMJ does not warrant the accuracy and reliability of the translations (including but not limited to local regulations, clinical guidelines, terminology, drug names and drug dosages), and is not responsible for any error and/or omissions arising from translation and adaptation or otherwise.

Open access This is an open access article distributed in accordance with the Creative Commons Attribution Non Commercial (CC BY-NC 4.0) license, which permits others to distribute, remix, adapt, build upon this work non-commercially, and license their derivative works on different terms, provided the original work is properly cited, appropriate credit is given, any changes made indicated, and the use is non-commercial. See: <http://creativecommons.org/licenses/by-nc/4.0/>.

ORCID iDs

Jessica Da Gama Duarte <http://orcid.org/0000-0003-4289-5204>

Lisa A Mielke <http://orcid.org/0000-0002-9522-9320>

REFERENCES

- Danpanichkul P, Suparan K, Tothnarungroj P, *et al*. Epidemiology of gastrointestinal cancers: a systematic analysis from the Global Burden of Disease Study 2021. *Gut* 2024;74:26–34.
- Lyu Y, Xie F, Chen B, *et al*. The nerve cells in gastrointestinal cancers: from molecular mechanisms to clinical intervention. *Oncogene* 2024;43:77–91.
- Sexton RE, Al Hallak MN, Diab M, *et al*. Gastric cancer: a comprehensive review of current and future treatment strategies. *Cancer Metastasis Rev* 2020;39:1179–203.
- Wang W, Li L, Chen N, *et al*. Nerves in the Tumor Microenvironment: Origin and Effects. *Front Cell Dev Biol* 2020;8:601738.
- Balood M, Ahmadi M, Eichwald T, *et al*. Nociceptor neurons affect cancer immunosurveillance. *Nature New Biol* 2022;611:405–12.
- Zhi X, Wu F, Qian J, *et al*. Nociceptive neurons promote gastric tumour progression via a CGRP-RAMP1 axis. *Nature New Biol* 2025;640:802–10.
- Furness JB. The enteric nervous system and neurogastroenterology. *Nat Rev Gastroenterol Hepatol* 2012;9:286–94.
- Furness JB, Rivera LR, Cho H-J, *et al*. The gut as a sensory organ. *Nat Rev Gastroenterol Hepatol* 2013;10:729–40.
- Yang D, Jacobson A, Meerschaert KA, *et al*. Nociceptor neurons direct goblet cells via a CGRP-RAMP1 axis to drive mucus production and gut barrier protection. *Cell* 2022;185:4190–205.
- Russo AF, Hay DL. CGRP physiology, pharmacology, and therapeutic targets: migraine and beyond. *Physiol Rev* 2023;103:1565–644.
- Labastida-Ramirez A, Caronna E, Gollion C, *et al*. Mode and site of action of therapies targeting CGRP signaling. *J Headache Pain* 2023;24:125.
- Wang K, Yaghi OK, Spallanzani RG, *et al*. Neuronal, stromal, and T-regulatory cell crosstalk in murine skeletal muscle. *Proc Natl Acad Sci U S A* 2020;117:5402–8.
- Iyengar S, Ossipov MH, Johnson KW. The role of calcitonin gene-related peptide in peripheral and central pain mechanisms including migraine. *Pain* 2017;158:543–59.
- Lai NY, Musser MA, Pinho-Ribeiro FA, *et al*. Gut-Innervating Nociceptor Neurons Regulate Peyer's Patch Microfold Cells and SFB Levels to Mediate Salmonella Host Defense. *Cell* 2020;180:33–49.
- Wallrapp A, Burkett PR, Riesenfeld SJ, *et al*. Calcitonin Gene-Related Peptide Negatively Regulates Alarmin-Driven Type 2 Innate Lymphoid Cell Responses. *Immunity* 2019;51:709–23.
- Zhao C-M, Hayakawa Y, Kodama Y, *et al*. Denervation suppresses gastric tumorigenesis. *Sci Transl Med* 2014;6:250ra115.
- Dömötör A, Peidl Z, Vincze Á, *et al*. Immunohistochemical distribution of vanilloid receptor, calcitonin-gene related peptide and substance P in gastrointestinal mucosa of patients with different gastrointestinal disorders. *Inflammopharmacol* 2005;13:161–77.
- Şerban R-E, Stepan M-D, Florescu DN, *et al*. Expression of Calcitonin Gene-Related Peptide and Calcitonin Receptor-like Receptor in Colorectal Adenocarcinoma. *Int J Mol Sci* 2024;25:4461.
- Anaya J. OncoLnc: linking TCGA survival data to mRNAs, miRNAs, and lncRNAs. *PeerJ Comput Sci* 2016;2:e67.
- Diaz Del Arco C, Fernández Aceñero MJ, Ortega Medina L. Molecular Classifications in Gastric Cancer: A Call for Interdisciplinary Collaboration. *Int J Mol Sci* 2024;25:2649.
- Lauren T. THE TWO HISTOLOGICAL MAIN TYPES OF GASTRIC CARCINOMA: DIFFUSE AND SO-CALLED INTESTINAL-TYPE CARCINOMA. AN ATTEMPT AT A HISTO-CLINICAL CLASSIFICATION. *Acta Pathol Microbiol Scand* 1965;64:31–49.
- The human protein atlas. Available: https://www.proteinatlas.org/ENSG00000132329-RAMP1/tissue#rna_expression
- Armaghany T, Wilson JD, Chu Q, *et al*. Genetic alterations in colorectal cancer. *Gastrointest Cancer Res* 2012;5:19–27.
- Barretina J, Caponigro G, Stransky N, *et al*. The Cancer Cell Line Encyclopedia enables predictive modelling of anticancer drug sensitivity. *Nature New Biol* 2012;483:603–7.
- The Cancer Genome Atlas Research Network. Comprehensive molecular characterization of gastric adenocarcinoma. *Nature New Biol* 2014;513:202–9.
- Nakamura Y, Kawazoe A, Lordick F, *et al*. Biomarker-targeted therapies for advanced-stage gastric and gastro-oesophageal junction cancers: an emerging paradigm. *Nat Rev Clin Oncol* 2021;18:473–87.
- Ooi CH, Ivanova T, Wu J, *et al*. Oncogenic pathway combinations predict clinical prognosis in gastric cancer. *PLoS Genet* 2009;5:e1000676.
- Gullo I, Grillo F, Mastracci L, *et al*. Precancerous lesions of the stomach, gastric cancer and hereditary gastric cancer syndromes. *Pathologica* 2020;112:166–85.
- Jeon T-Y, Han M-E, Lee Y-W, *et al*. Overexpression of stathmin1 in the diffuse type of gastric cancer and its roles in proliferation and migration of gastric cancer cells. *Br J Cancer* 2010;102:710–8.
- Qi Y, Xu R. Roles of PLODs in Collagen Synthesis and Cancer Progression. *Front Cell Dev Biol* 2018;6:66.
- Lan J, Zhang S, Zheng L, *et al*. PLOD2 promotes colorectal cancer progression by stabilizing USP15 to activate the AKT/mTOR signaling pathway. *Cancer Sci* 2023;114:3190–202.
- Kim M, Jang K, Miller P, *et al*. VEGFA links self-renewal and metastasis by inducing Sox2 to repress miR-452, driving Slug. *Oncogene* 2017;36:5199–211.
- Yu Q, Fu W, Fu Y, *et al*. BNIP3 as a potential biomarker for the identification of prognosis and diagnosis in solid tumours. *Mol Cancer* 2023;22:143.
- Du J, Yang M, Chen S, *et al*. PDK1 promotes tumor growth and metastasis in a spontaneous breast cancer model. *Oncogene* 2016;35:3314–23.
- Yu G, Huang B, Chen G, *et al*. Phosphatidylethanolamine-binding protein 4 promotes lung cancer cells proliferation and invasion via PI3K/Akt/mTOR axis. *J Thorac Dis* 2015;7:1806–16.
- Wang X, Guo J, Dai M, *et al*. PLOD2 increases resistance of gastric cancer cells to 5-fluorouracil by upregulating BCRP and inhibiting apoptosis. *J Cancer* 2020;11:3467–75.
- Liu Z, Li L, Liu L. PDK3 drives colorectal carcinogenesis and immune evasion and is a therapeutic target for boosting immunotherapy. *Am J Cancer Res* 2024;14:3117–29.

- 38 Li L, Li L, Li W, *et al.* TAp73-induced phosphofructokinase-1 transcription promotes the Warburg effect and enhances cell proliferation. *Nat Commun* 2018;9:4683.
- 39 Wang XQ, Fan AQ, Hong L. LncRNA MIR210HG promotes the proliferation of colon cancer cells by inhibiting ferroptosis through binding to PCBP1. *Sci Rep* 2025;15:871.
- 40 Sui Y, Jiang H, Kellogg CM, *et al.* Promotion of colorectal cancer by transcription factor BHLHE40 involves upregulation of ADAM19 and KLF7. *Front Oncol* 2023;13:1122238.
- 41 Zhou Y, Zhou B, Pache L, *et al.* Metascape provides a biologist-oriented resource for the analysis of systems-level datasets. *Nat Commun* 2019;10:1523.
- 42 Zahalka AH, Frenette PS. Nerves in cancer. *Nat Rev Cancer* 2020;20:143–57.
- 43 Jiang S-H, Hu L-P, Wang X, *et al.* Neurotransmitters: emerging targets in cancer. *Oncogene* 2020;39:503–15.
- 44 Weinberg BA, Marshall JL. Colon Cancer in Young Adults: Trends and Their Implications. *Curr Oncol Rep* 2019;21:3.
- 45 Nagashima H, Mahlaköiv T, Shih H-Y, *et al.* Neuropeptide CGRP Limits Group 2 Innate Lymphoid Cell Responses and Constrains Type 2 Inflammation. *Immunity* 2019;51:682–95.
- 46 Xu H, Ding J, Porter CBM, *et al.* Transcriptional Atlas of Intestinal Immune Cells Reveals that Neuropeptide α -CGRP Modulates Group 2 Innate Lymphoid Cell Responses. *Immunity* 2019;51:696–708.
- 47 Huang Q, Jacquolot N, Preaudet A, *et al.* Type 2 Innate Lymphoid Cells Protect against Colorectal Cancer Progression and Predict Improved Patient Survival. *Cancers (Basel)* 2021;13:559.
- 48 O’Keefe RN, Carli ALE, Baloyan D, *et al.* A tuft cell - ILC2 signaling circuit provides therapeutic targets to inhibit gastric metaplasia and tumor development. *Nat Commun* 2023;14:6872.
- 49 Darragh LB, Nguyen A, Pham TT, *et al.* Sensory nerve release of CGRP increases tumor growth in HNSCC by suppressing TILs. *Med* 2024;5:254–70.
- 50 Kaminishi M, Shimizu N, Shimoyama S, *et al.* Denervation promotes the development of cancer-related lesions in the gastric remnant. *J Clin Gastroenterol* 1997;25 Suppl 1:S129–34.
- 51 Messina R, Huessler E-M, Puledda F, *et al.* Safety and tolerability of monoclonal antibodies targeting the CGRP pathway and gepants in migraine prevention: A systematic review and network meta-analysis. *Cephalalgia* 2023;43:3331024231152169.
- 52 Huber A, Allam AH, Dijkstra C, *et al.* Mutant TP53 switches therapeutic vulnerability during gastric cancer progression within interleukin-6 family cytokines. *Cell Rep* 2024;43:114616.
- 53 Thilakasiri P, O’Keefe RN, To SQ, *et al.* Mechanisms of cellular crosstalk in the gastric tumor microenvironment are mediated by YAP1 and STAT3. *Life Sci Alliance* 2024;7:e202302411.
- 54 Williams DS, Mouradov D, Browne C, *et al.* Overexpression of TP53 protein is associated with the lack of adjuvant chemotherapy benefit in patients with stage III colorectal cancer. *Mod Pathol* 2020;33:483–95.
- 55 Williams DS, Mouradov D, Jorissen RN, *et al.* Lymphocytic response to tumour and deficient DNA mismatch repair identify subtypes of stage II/III colorectal cancer associated with patient outcomes. *Gut* 2019;68:465–74.
- 56 Tan T, Mouradov D, Gibbs P, *et al.* Protocol for generation of and high-throughput drug testing with patient-derived colorectal cancer organoids. *STAR Protoc* 2024;5:103090.
- 57 Liao Y, Smyth GK, Shi W. The Subread aligner: fast, accurate and scalable read mapping by seed-and-vote. *Nucleic Acids Res* 2013;41:e108.
- 58 Liao Y, Smyth GK, Shi W. The R package Rsubread is easier, faster, cheaper and better for alignment and quantification of RNA sequencing reads. *Nucleic Acids Res* 2019;47:e47.
- 59 Liao Y, Smyth GK, Shi W. featureCounts: an efficient general purpose program for assigning sequence reads to genomic features. *Bioinformatics* 2014;30:923–30.
- 60 Law CW, Chen Y, Shi W, *et al.* voom: Precision weights unlock linear model analysis tools for RNA-seq read counts. *Genome Biol* 2014;15:R29.
- 61 Ritchie ME, Phipson B, Wu D, *et al.* limma powers differential expression analyses for RNA-sequencing and microarray studies. *Nucleic Acids Res* 2015;43:e47.
- 62 Smyth GK. Linear models and empirical bayes methods for assessing differential expression in microarray experiments. *Stat Appl Genet Mol Biol* 2004;3:Article3.